

ANALYSIS OF A DSM GENERATION ALGORITHM FOR THE ADS40 AIRBORNE PUSHBROOM SENSOR

Maria PATERAKI and Emmanuel BALTSAVIAS

Institute of Geodesy and Photogrammetry, ETH Zurich, Switzerland

[\(maria,manos\)@geod.baug.ethz.ch](mailto:(maria,manos)@geod.baug.ethz.ch)

KEY WORDS: ADS40, airborne digital sensor, DSM, matching, quantitative analysis

ABSTRACT

In this paper, a thorough analysis on automatic DSM generation from imagery, acquired by the airborne pushbroom sensor ADS40, is presented. At first, the algorithmic approach is described, focusing on its essential key components that exploit the special geometric and radiometric characteristics of the sensor and thus facilitate automatic extraction of 3D information. The novel algorithm makes use of a multi-image, multi-template approach with geometrical constraints. These constraints make use of quasi-epipolar lines, since each line has its own position and attitude, to restrict search space. The multi-template approach uses more than one template images, while matching is performed in pairwise mode, aiming at reducing problems occurring due to occlusions. In addition to the above, feature-based and area-based approaches are used, where edges with attributes, extracted points (edgels) and grid points are matched to generate a dense DSM. Experimental results of automatic DSM generation are derived from an ADS40 dataset acquired over Waldkirch, Switzerland and are further quantitatively analyzed and compared with respect to the single-, multi-template strategy, the type of matched points utilized in the algorithm, as well as the landcover. Reference data, used in this assessment have been collected by manual measurements of mass points from the ADS40 dataset. Therefore, error sources like conversions among different coordinates systems, multi-temporal differences between datasets and geometrical accuracy of sensor orientation do not influence the analysis of the results, and thus the comparison reflects purely the internal matching accuracy. In order to take into account the effect of landcover in the analysis, DSMs have been extracted in three test areas of different landcover type. Reference data have been further separated into three classes of bare ground, man-made objects and trees and statistical values are derived for the above classes.

1 INTRODUCTION

1.1 State of the art

The rapid technological developments of the 90's have completely redefined the mapping practice as a whole. In less than a decade, digital techniques have come to outnumber the traditionally analog processing methods. Supported by unprecedented demand for large volume and accurate spatial data, these new digital techniques emerged as dominant mapping technologies by the end of the decade. The technological change has recently also reached the analog-camera based aerial surveying practice, which supplies about two-thirds of spatial data for mapping and was the last stronghold of analog techniques. Two key components of this emerging technology are the electronic-sensor-based digital cameras and the GPS/INS- based direct platform orientation. Single- and multi-line CCDs are employed as research tools in satellite- and airborne- based sensors and are used to acquire panchromatic and multispectral imagery in pushbroom mode for photogrammetric and remote sensing applications. Regarding airborne sensors, several systems have been developed and among them fewer commercial ones, e.g. ADS40 (LH Systems), DMC (Z/I Imaging), TLS

(Starlabo), Ultracam-D (Vexcel). New methods, compared to the existing ones for processing of scanned aerial films, are necessary for digital sensors, especially line-CCD-based ones. In fact they have significant differences to the existing film-based cameras, e.g. several (up to 9) CCD-lines with 100% overlap, a non-perspective geometry in flight direction, different radiometric characteristics, simultaneous multispectral imaging capabilities, more complicated imaging geometry and integration of GPS/INS systems for determination of the position and orientation of each line. Investigations regarding airborne linear-CCDs have been already performed regarding camera architecture, direct georeferencing, sensor modeling, ground processing and aerial triangulation for ADS40 (Fricker, 2001; Hinsken et al., 2002; Sandau et al., 2000; Tempelmann et al., 2000) and for other systems (Fritsch, 1997; Haala et al., 2000; Hoffmann et al., 2000; Leberl et al., 2003; Tianen et al., 2003; Wewel et al., 1998). Less is published though on matching methods and DSM generation using airborne linear CCDs and even less details are given on the algorithms employed (Gwinner et al., 1999; Neukum, 1999, Scholten, 2000).

1.2 Characteristics of ADS40

A detailed description of the camera system and the architecture of ADS40 already exist in the literature (Reulke et al., 2000; Sandau et al., 2000, Tempelmann et al., 2000). In brief, ADS40 consists of seven parallel sensor lines in the focal plane of a single lens system – three panchromatic (forward, nadir, backward), red, green, and blue lines placed next to each other and one infrared (Figure 1) and incorporates GPS and INS technology (Applanix).

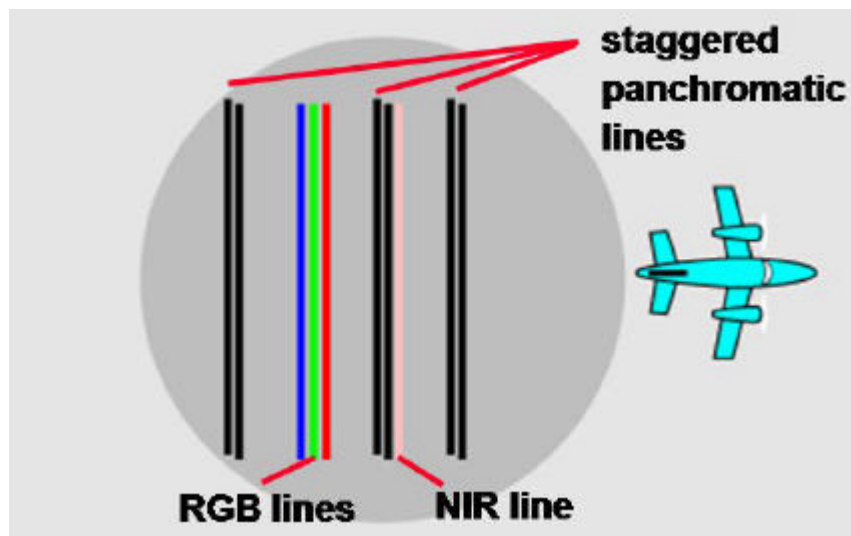


Figure 1. Configuration of channels on ADS40

Each panchromatic channel consists of two lines, each with 12000 pixels, staggered by 0.5 pixels. The color and near-infrared channels can support a better interpretation of imagery, classification of vegetation and man-made objects and their use can assist and facilitate automatic object recognition and extraction. Their use in the extraction of homologous features is of advantage from both a radiometric and geometric point of view.

1.2.1 Geometric characteristics. In general, with line-CCDs the images overlap 100% (with frame imagery typically only 60%), while the perspective distortions in the flight direction are small due to the quasi parallel projection. The problem of different image scale in flight direction is reduced when processing rectified ADS40 images. ADS40 channels are rectified onto a height plane (Lev1 images) and therefore differences due to scale, but also rotation and shear that exist in raw images (Lev 0 images) are removed to a large extent. Rectified images are used for stereo viewing and also

in the matching process for tie point extraction and DSM/DTM generation. All CCD lines on the focal plane, panchromatic and multispectral, at an instant of time t have their own position and attitude, different viewing angles and calibration, which leads to a more complicated imaging geometry, compared to frame imagery. Geometric transformations can be more complex, however a sufficient accuracy can be achieved by direct georeferencing, using a GPS/INS system, and subsequent improvement of orientation and calibration using GCPs.

The use of multiple channels can increase reliability and accuracy of matching results and the different viewing angles help to disambiguate difficult matching cases and thus generate reliable photogrammetric products, reducing manual postprocessing.

1.2.2 Radiometric characteristics. ADS40 data have a dynamic range of up to 14 bits [0 – 16384 GV's] (versus the usual 8 bits [0-255 GV's] of frame imagery) and exhibit a very good signal to noise ratio. The effective number of bits is less in the red, green and blue channels. Histograms of raw (Lev 0) images show a strong peak towards the darker grey values (about 310-340 in the panchromatic channels). The radiometric characteristics were analyzed for various datasets acquired in the last two years and the noise analysis that has been performed, based on the algorithm described in Baltasvias et al. (2001) indicated that noise is generally low (standard deviation is about 2 grey values), and intensity dependent. A more detailed analysis can be found in Pateraki et al. (2002).

2 DSM EXTRACTION

2.1 General matching strategy

Most of existing matching algorithms are geared towards frame aerial imagery, while in matching only two images are used. However, for ADS40 a multi-image matching approach can be followed, leading to substantial reduction of problems caused by occlusions, multiple solutions, image noise, and surface discontinuities. Moreover higher measurement accuracy can be achieved through the intersection of more than two image rays. Besides this, geometric constraints can be enforced and restrict the search space along quasi-epipolar lines, using the known sensor model implemented by LGGM (Leica Geosystems GIS and Mapping). Rectified images are used mainly for DSM extraction for which the epipolar curve can be approximated by a line and the solution can be constrained along the epipolar line. It has been observed that these images generally exhibit small scale and rotation differences, especially in the upper pyramid levels, where the use of only shifts in matching, without additional shaping parameters (e.g. scales and shears in Least Squares Matching (LSM)), is justified, reducing therefore processing time.

In the first tests, the algorithm was applied only on extracted edge pixels, derived by the Canny operator (one pixel wide edges) or the "gradient thresholding" operator (in-house developed algorithm, more than one pixel wide edges), using gray level images, and a multi-patch approach (pixel accuracy) with normalized cross correlation as similarity measure. Least squares matching (sub-pixel accuracy) is employed in the quality control only for those points, for which correlation matching indicated that were successful candidates depending on their computed quality measures. Since matching is performed in pairwise mode, to detect problems occurring in individual images, the quality measures are used for each image ray. Weak rays are excluded and final 3D intersection is computed using only the good rays (more detailed description for general strategy and automatic error detection and in Pateraki et al., 2003).

Geometrical constraints are used in the multi-patch as well as in the LSM approach in order to decrease the processing time and increase the reliability of the solution. For example, in texture with repetitive patterns (e.g. agricultural fields) the constrained approach has a higher success rate (solution is both precise and reliable), compared to the unconstrained one (solution might converge but not always reliable), since less possible candidates exist. Figure 2 illustrates the processing steps

of the above mentioned strategy. Along breaklines some extracted points are rejected, due to the fact that discontinuities can not be fully modeled by single point area-based matching. As a result, the modeling of the surface is partially incomplete. To solve this problem, matching has been extended to edge features with attributes (e.g. length, orientation, strength, etc.) and as an option, additional extracted features or grid points can be included in the matching process. Grid points are used in conjunction with larger masks in cases of areas with less texture. However mask size should not exceed certain limits or/and include information that can not be modeled by LSM (e.g. points close to buildings in shadowed areas).

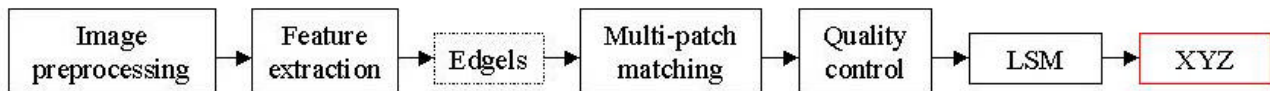


Figure 2. Strategy for single point area-based matching (edgels)

As mentioned before matching is performed in pairwise mode. A single or multi-template strategy can be utilized in the matching process. In single template strategy only one image is utilized as template and all remaining images are used as patches (commonly the nadir channel is used as template). The multi-template strategy is justified since one template may not suffice to detect and avoid problems occurring in matching, especially occlusions. ADS40 permits with the given configuration of line CCDs to use more than one template and thus facilitates the identification of errors. Detailed information about possible combinations of channels and their role in image matching can be found in Pateraki et al. (2003).

2.2 Edge extraction

The Lev1 images are processed with an adaptive filtering (Baltasvias et al., 2001) to reduce noise, then with the Wallis filter (Wallis, 1976) to enhance contrast and radiometrically balance the images. Single extracted edgels have to be linked into contours. The edgel aggregation is a sequential process, where the significant contours are aggregated before the weaker ones (Henricsson, 1996) and small gaps are bridged based on criteria of proximity and collinearity. After the contour graph is generated, it is postprocessed based on defined attributes to remove weak contours and obtain as long and straight contours as possible. The attributes can be geometrical (e.g. length, curvature of contour), radiometrical (e.g. strength of edge) or topological (e.g. adjacency, common end points). In Figure 3, the extracted edgels, the initially linked contours and the postprocessed contours with the attributes extracted from the nadir channel are displayed.

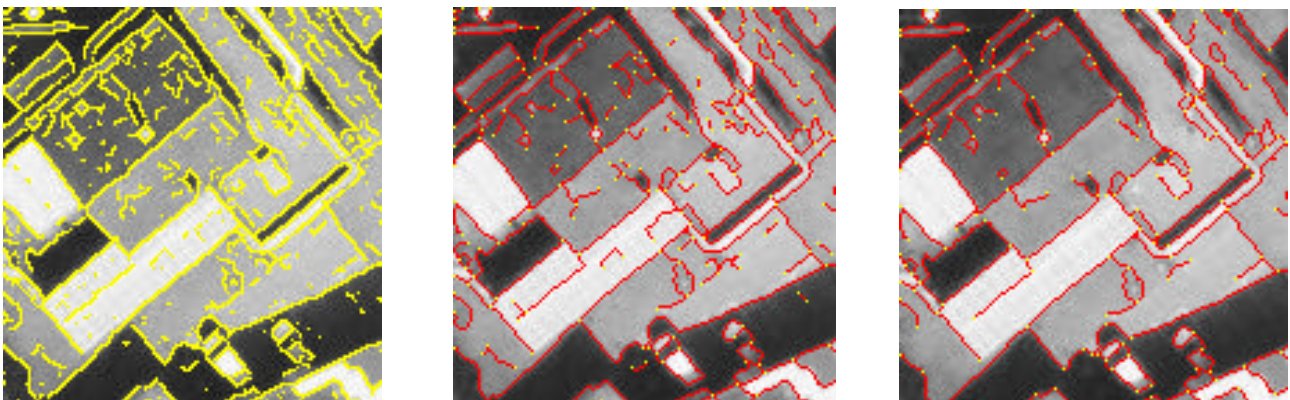


Figure 3. On the left, extracted edgels with the Canny operator. In the middle, the initially linked contours. On the right, the postprocessed contours. The bright pixels along the contour (middle and right) indicate the vertices and the darker ones the contour pixels.

During postprocessing some weak edges might be excluded but the advantage is that contours do not belong to different objects (possibly of different height). In the above approach, edge vertices are matched first. Then, points that lie on each contour are matched sequentially with an approximation of height, derived from the 3D coordinates of the vertices and the length of the contour. Contours can support better representation of discontinuities compared to single point matching. However, for DSM generation additional points are required to fill possible gaps. Therefore, in the matching process extracted grid points and/or non linked edges are introduced in the lower image pyramid levels, where an approximation of the surface already exists. In this way, robust (due to continuity and height constraint along the edge) approximations are derived in the upper levels faster, supporting a denser extraction in the lower levels. Edges are extracted in the template image and the single template strategy is selected for the matching. Multi template strategy can be also used as an option where edgels are aggregated in the first template and if template changes then single point matching is used on the second template. If edgels were aggregated on both templates, employing the current approach, then vertices and contour points would have to be matched separately from each template in order to maintain the topology and they would result in a time consuming program. For this reason, multi template strategy for edges will need to be developed on a different concept. Additional points that are introduced in later stages of matching can be matched either with single- or multi-template strategy (see Figure 4).

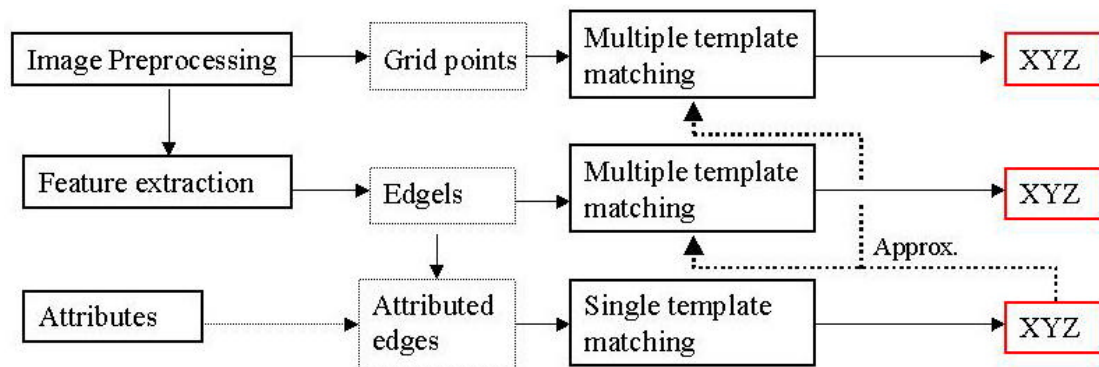


Figure 4. Example scheme for image matching including edges with attributes, edgels and grid points. Single template strategy can be also used for edgels and grid points instead of multi template.

2.3 Initial approximations for shaping parameters

Integration of edges requires that the height of the vertices has to be computed as accurately as possible, since this information is used for derivation of initial approximations for the connected points along the contour to which the vertex (closed contour) or vertices (open contours) belong. Therefore, sub-pixel accurate matching results have to be derived. In LSM, initial approximations for the four shaping parameters (scales and shears) can be estimated by analysing the signal in the patches (template and patch), thus increasing success and convergence rate. Since edgels have high intensity gradients across the edge direction the error ellipse will not be isotropic and initial shaping parameters for the patches can be computed from differences in edge direction and the ratios of semi-major and semi-minor axes of the signal ellipse of template and patch (Figure 5).

Thus, approximate position is required and can be obtained by the multi-patch approach. Tests showed that for single point matching with and without a priori estimation of the shaping parameters, iterations decreased by a factor of three and success rate increased (35% for 20 match points).



Figure 5. On the left, in the middle, on the right the error ellipses for a point on Backward, Nadir and Forward channel respectively. The values for the error ellipses have been calculated out of a patch 15 x 15 centered on the given point (cross).

3 EXPERIMENTAL RESULTS

3.1 Dataset

The processed dataset was acquired over the region of Waldkirch in Switzerland in May 2002 and included panchromatic and multispectral imagery. A block of images has been delivered including four parallel and two cross strips. Only rectified (Lev1) images from one strip have been used till now, with a ground sampling distance of 0.21 m. The coordinates were defined in WGS84. In order to evaluate the algorithmic performance for DSM generation and the internal matching accuracy, manually collected mass points from the ADS40 imagery have been used as reference data and have been classified to: (i) bare ground (BE), (ii) man-made objects (MMO) and (iii) trees (T). An analysis has been performed for the 3 separate classes. DSMs have been extracted in 3 test regions of different landcover: (a) bare ground, (b) bare ground and forest, (c) bare ground and man-made objects. All test regions, illustrated in Figure 6, had a smooth terrain relief. The size of area A, B and C was 2000 x 1000, 1500 x 1000 and 1500 x 1500 pixels respectively.



Figure 6. On the left, in the middle, on the right the test areas A, B and C respectively. Images have been processed (brightened) for visualization purposes.

3.2 Strategies and analysis

In previous tests (Pateraki et. al, 2003), accuracy increased with the number of images used (significant improvement when using three instead of two images, less when using four instead of three). The backward, nadir and forward channels were used in all tests. The analysis focuses on the

comparison of the strategies (single-, multi-template) as well as how different selected features for matching (edges, edgels, grid,) influence the accuracy of the result. In the single template strategy, the nadir channel has been used as template and in the multi-template strategy the outer channels (in this case, backward and forward panchromatic). In all tests, five pyramid levels combined with doublet strategy (Pateraki et al. 2003) were used. Raw DSM points without any postprocessing (e.g. filtering, modeling of breaklines) and interpolated elevations of the reference-measured points were utilized to compute elevation differences (mean with sign, standard deviation and RMS). Landcover variation in the three test areas justified the use of different strategies in terms of template and feature selection. In area A, single- and multi-image strategies have been applied on extracted edgels and the single template strategy on grid points with a predefined step of 5 pixels which corresponds approximately to 1m on the ground (Table 1).

	Single template strategy						Multi-template strategy		
	Edgels (308000)			Grid (60000)			Edgels (367000)		
	mean	RMS	St. Dev.	mean	RMS	St. Dev.	mean	RMS	St. Dev.
BE (100)	0.18	0.45	0.36	0.17	0.43	0.34	0.27	0.45	0.29

Table 1. Quantitative analysis of matching accuracy in test area A with respect to the selection of matching strategy (in parenthesis the matched points). Compared with bare earth (BE), where in parenthesis the interpolated points. All statistical measures of differences are in m.

In view of the fact that the terrain was smooth (no discontinuities) and relatively many features have been extracted in the agricultural fields due to contrast enhancement, computation of edges with attributes was meaningless as well as costly. Multi template strategy derived better results compared to the other but in terms of time, extraction and matching of grid points was faster compared to edge pixels (even with higher thresholds for Canny many features have been extracted due to contrast enhancement that has been applied in the whole image with constant parameters for all areas).

Test area B included complex objects (small and large building blocks, trees close to roofs, etc.). Besides, a few or no points have been extracted in shadowed areas close to the base of buildings. The integration of edges with attributes was of an advantage in the representation of discontinuities, since points on the perimeter of buildings (contour points) were not only constrained along the epipolar line but also within the computed height range, derived from the successfully matched vertices. First, only edges with attributes have been matched and identical points were compared with 100 measured roof corners. The mean Z difference was -0.33 m and the RMS was 0.65 m. Even though points have been successfully matched still some were rejected (by automatic error detection) due to the fact that the geometrical differences between template and patch could not be modeled by the affine transformation in LSM. Unlinked edgels and grid points have been used in the lower levels (1 and 0) to generate a denser surface.

As it can be seen in the analysis (Table 2) when all man-made objects were included, accuracy degraded since some points along building outlines were rejected by automatic error detection and therefore elevation was interpolated from the nearest points which apparently were on the ground or on near-by edges. Therefore these interpolated elevations were indicated as blunders in the analysis but in reality not enough points have been successfully matched. It is also apparent that the difference in landcover compared to test area A decreased the accuracy even when results are only compared with bare earth (BE). This is due to the fact that the object surface is more complex, without many open areas as in test area A. As it was expected, accuracy improves for the multi-template approach. Grid points deliver similar results but faster compared to edgels for both multi and single template strategies.

	Single template						Mult. templates					
	Edgels (62000)			Grid (23000)			Edgels (65300)			Grid (26456)		
	mean	RMS	St. Dev	mean	RMS	St. Dev	mean	RMS	St. Dev	mean	RMS	St. Dev
BE (80)	0.14	0.68	0.64	0.13	0.67	0.63	0.12	0.64	0.60	0.11	0.62	0.55
MMO (350)	0.50	1.17	0.93	0.48	1.14	0.90	0.42	1.07	0.86	0.39	1.02	0.82

Table 2. Quantitative analysis of matching accuracy in test area B with respect to the selection of matching strategy. Edgels and/or grid points have been included in addition to edges with attributes. All results in meters.

In general, for this type of area, it is proposed to extract an approximate DSM in the upper pyramid levels using edges with attributes to derive a better approximation of discontinuities (coarser but more accurate compared to grid) and then subsequently densify in the lower levels with grid points (faster compared to edgels).

In the case of test area C, the accuracy decreased ($RMS > 1.5$ m for class T), as expected, since trees were included and are considered to be one of the most difficult matching cases. Comparison with BE derived similar results as in test area A since a large part of open area was included in test area C.

4 CONCLUSIONS AND FUTURE WORK

ADS40 imagery enables the use of a multi-image approach with quasi-epipolar constraints in matching. In addition to this, the promising concept of multiple templates makes use of the special characteristics of the sensor. A combined approach of feature-based and area-based matching is implemented. The use of edges with attributes improves overall the result when buildings are included in the DSM. In terms of processing time, it is favorable to extract an approximate DSM, using edge features and then fill possible gaps and improve its quality and representation of the surface by the inclusion of grid points. On one hand are more suitable to fill gaps in areas where less points have been extracted (weak signal) but also to represent a smooth surface with a reasonable amount of points and therefore decrease processing time. Future work will be concentrated on more detailed aspects of edge matching for building outlines (e.g. LSM for straight edge features) and on the modeling of breaklines.

ACKNOWLEDGEMENTS

This work was performed within the project AIM, a cooperation of ETH Zurich and LGGM (Leica Geosystems GIS and Mapping). The general support of the ADS40 development team of LGGM is gratefully acknowledged.

REFERENCES

Baltsavias E., Pateraki M., Zhang L., 2001. Radiometric and Geometric Evaluation of IKONOS Geo Images and their use for 3D building modelling. Proc. Joint ISPRS Workshop "High Resolution Mapping from Space 2001", Hannover, Germany, 19-21 September (on CD-ROM).

- Börner A., Reulke R., 2001. Results of Test Flights with the Airborne Digital Sensor ADS40. In: R. Klette, S. Peleg, G. Sommer (Eds.), International Workshop RobVis 2001, Springer 2001, ISBN 3-540-41694-3, pp. 270-277.
- Fricker P., 2001. ADS40 – Progress in digital aerial data collection. In: D. Fritsch, R. Spiller (Eds.), Photogrammetric Week '01, Wichmann Verlag, Heidelberg, pp. 105 - 116.
- Fritsch D., 1997. Experiences with the Airborne Three-line Photogrammetric Image Acquisition System DPA. In: D. Fritsch, D. Hobbie (Eds.), Photogrammetric Week '97, Wichmann Verlag, Heidelberg, pp. 63-74.
- Gwinner K., Hauber E., Hoffmann H., Scholten F., Jaumann R., Neukum G., Puglisi G., Coltelli M., 1999. The HRSC-A Experiment on High Resolution Multispectral Imaging and DEM Generation at the Aeolian Islands. 13th Int. Conf. on Applied Geologic Remote Sensing, Vancouver B.C., March 1999, Vol. I, pp. 560-569.
- Haala N., Fritsch D., Stallmann D., Cramer M., 2000. On the performance of digital airborne pushbroom cameras for photogrammetric data processing - a case study. In: *Int'l Archives of Photogrammetry and Remote Sensing*, Vol. 33, Part B4/1, pp. 324-331.
- Henricsson, O., 1996. Analysis of Image Structure using Color Attributes and Similarity Relations. Ph.D. Thesis, Report No.59, Institute of Geodesy and Photogrammetry, ETH Zurich, Switzerland.
- Hinsken L., Miller S., Tempelmann U., Uebbing R., Walker S., 2001. Triangulation of LH Systems' ADS40 imagery using ORIMA GPS/IMU. In: *Int'l Archives of Photogrammetry and Remote Sensing*, Vol. 34, Part B3/A, pp. 156-162.
- Hoffmann A., van der Vegt J.W., Lehmann F. 2000. Towards automated map updating: Is it feasible with new digital data-acquisition and processing techniques?. In: *Int'l Archives of Photogrammetry and Remote Sensing*, Vol. 33, Part B2, pp. 295-302.
- Leberl W.F., Gruber M., Ponticelli M., Bernoegger S., Perko R., 2003. The UltraCam Large Format Aerial Digital Camera System. Proc. ASPRS Annual Conference 2003, (on CD-ROM).
- Neukum G., 1999. The Airborne HRSC-A: Performance Results and Application Potential. In: Photogrammetric Week '99, D. Fritsch, D. Hobbie (Eds.), Wichmann, Heidelberg, pp. 83-88.
- Pateraki M., Baltsavias E., 2002. Adaptive Multi-Image Matching Algorithm for the Airborne Digital Sensor ADS40. Proc. Map Asia 2002, Asian Conference on GIS, GPS, Aerial Photography and Remote Sensing, (on CD-ROM).
- Pateraki M., Baltsavias E., 2003. Analysis and performance of the Adaptive Multi-Image matching algorithm for airborne digital sensor ADS40. Proc. ASPRS Annual Conference 2003, (on CD-ROM).
- Reulke, R., Franke, K., Pomierski, T., Schönermark, M., Tornow, C., Wiest, L., 2000. Target related multispectral and true colour optimization of the colour channels of the LH Systems ADS40. *Int'l Archives of Photogrammetry and Remote Sensing*, Vol. 33, Part B1, pp. 244-250.
- Sandau, R., Braunecker B., Driescher, H., Eckardt, A., Hilbbert, S., Hutton, J., Kirchhofer, W., Lithopoulos, E., Reulke, R., Wicki, S., 2000. Design principles of the LH Systems ADS40 airborne digital sensor. *Int'l Archives of Photogrammetry and Remote Sensing*, Vol. 33, Part B1, pp. 258-265.
- Scholten F., 2000. Digital 3D data acquisition with the High Resolution Stereo Camera – Airborne (HRSC-A). In: *Int'l Archives of Photogrammetry and Remote Sensing*, Vol. 33, Part B4, pp. 901-908.
- Tempelmann, U., Börner, A., Chaplin, B., Hinsken, L., Mykhalevych, B., Miller, S., Recke, U., Reulke, R., Uebbing, R., 2000. Photogrammetric Software for the LH Systems ADS40 Airborne Digital Sensor. *Int'l Archives of Photogrammetry and Remote Sensing*, Vol. 33, Part B2, 552-559.
- Tianen C., Ryosuke S., Murai S., 2003. Development and Calibration of the Airborne Three-Line Scanner (TLS) Imaging System. *Photogr. Eng. and Rem. Sens.* 69(1), 71-78.

- Wallis R., 1976. An approach to the space variant restoration and enhancement of images. Proc. Of Symposium on Current Mathematical Problems in Image Science, Naval Postgraduate School, Monterey, CA, November.
- Wewel F., Scholten F., Neukum G., Albertz J., 1998. Digitale Luftbildaufnahme mit der HRSC – Ein Schritt in die Zukunft der Photogrammetrie. Photogrammetrie – Fernerkundung Geoinformation (6), 337-348.